

<https://helda.helsinki.fi>

Centrality dependence of the pseudorapidity density distribution for charged particles in Pb-Pb collisions at $\sqrt{s(NN)}=5.02$ TeV

Adam, J.

2017-09-10

Adam , J , Brucken , E J , Chang , B , Kim , D J , Litichevskyi , V , Mieskolainen , M M ,
Orava , R , Rak , J , Räsänen , S S , Snellman , T W , Trzaska , W H , Viinikainen , J & The
ALICE Collaboration 2017 , ' Centrality dependence of the pseudorapidity density distribution
for charged particles in Pb-Pb collisions at $\sqrt{s(NN)}=5.02$ TeV ' , Physics Letters B , vol.
772 , pp. 567-577 . <https://doi.org/10.1016/j.physletb.2017.07.017>

<http://hdl.handle.net/10138/231301>

<https://doi.org/10.1016/j.physletb.2017.07.017>

cc_by

publishedVersion

Downloaded from Helda, University of Helsinki institutional repository.

This is an electronic reprint of the original article.

This reprint may differ from the original in pagination and typographic detail.

Please cite the original version.



Centrality dependence of the pseudorapidity density distribution for charged particles in Pb–Pb collisions at $\sqrt{s_{\text{NN}}} = 5.02$ TeV

ALICE Collaboration ^{*}

ARTICLE INFO

Article history:

Received 9 January 2017

Received in revised form 19 June 2017

Accepted 9 July 2017

Available online 14 July 2017

Editor: L. Rolandi

ABSTRACT

We present the charged-particle pseudorapidity density in Pb–Pb collisions at $\sqrt{s_{\text{NN}}} = 5.02$ TeV in centrality classes measured by ALICE. The measurement covers a wide pseudorapidity range from -3.5 to 5 , which is sufficient for reliable estimates of the total number of charged particles produced in the collisions. For the most central (0–5%) collisions we find 21400 ± 1300 , while for the most peripheral (80–90%) we find 230 ± 38 . This corresponds to an increase of $(27 \pm 4)\%$ over the results at $\sqrt{s_{\text{NN}}} = 2.76$ TeV previously reported by ALICE. The energy dependence of the total number of charged particles produced in heavy-ion collisions is found to obey a modified power-law like behaviour. The charged-particle pseudorapidity density of the most central collisions is compared to model calculations – none of which fully describes the measured distribution. We also present an estimate of the rapidity density of charged particles. The width of that distribution is found to exhibit a remarkable proportionality to the beam rapidity, independent of the collision energy from the top SPS to LHC energies.

© 2017 The Author(s). Published by Elsevier B.V. This is an open access article under the CC BY license (<http://creativecommons.org/licenses/by/4.0/>). Funded by SCOAP³.

1. Introduction

In ultra-relativistic heavy-ion collisions a dense and hot phase of nuclear matter is created [1–4]. This phase of QCD matter is considered to be a plasma of strongly interacting quarks and gluons and is therefore labelled the sQGP [5]. The multiplicity of primary, charged particles produced in heavy-ion collisions is a key observable to characterise the properties of the matter created in these collisions [6]. The study of the primary charged-particle pseudorapidity density ($dN_{\text{ch}}/d\eta$) over a wide pseudorapidity (η) range and its dependence on colliding system, centre-of-mass energy, and collision geometry is important to understand the relative contributions to particle production from hard scatterings and soft processes, and may provide insight into the partonic structure of the interacting nuclei.

We have previously reported measurements on primary charged-particle pseudorapidity densities over a wide pseudorapidity range in Pb–Pb collisions at the centre-of-mass energy per nucleon pair $\sqrt{s_{\text{NN}}} = 2.76$ TeV [7]. In this Letter, we study these distributions in the pseudorapidity interval from -3.5 to 5 at a collision energy of $\sqrt{s_{\text{NN}}} = 5.02$ TeV as a function of the centrality. Pseudorapidity is defined as $\eta \equiv -\log(\tan(\vartheta/2))$, where ϑ is the angle between the charged-particle trajectory and the beam axis (z -axis). Nuclei are extended objects, and their collisions can be characterised by centrality – the experimental proxy for the un-measurable distance

between the centres of the colliding nuclei (impact parameter). A primary particle is a particle with a mean proper lifetime τ larger than $1 \text{ cm}/c$, which is either a) produced directly in the interaction, or b) from decays of particles with τ smaller than $1 \text{ cm}/c$, restricted to decay chains leading to the interaction [8]. In this Letter, all quantities reported are for primary charged particles, though we will omit “primary” for brevity.

With the large pseudorapidity coverage available in ALICE, we can reliably estimate, for all centrality classes, the total number of charged particles produced in the collisions. We therefore also present the first measurement of the total charged-particle multiplicity in Pb–Pb collisions at $\sqrt{s_{\text{NN}}} = 5.02$ TeV as a function of the number of nucleons participating in the collisions (N_{part}).

Finally, we transform the measured $dN_{\text{ch}}/d\eta$ distribution for the 5% most central collisions into charged-particle rapidity density (dN_{ch}/dy), and we examine the centre-of-mass energy dependence of the width of that distribution. The rapidity (y) of a particle with energy E and momentum component p_z along the beam axis is defined as $y \equiv \frac{1}{2} \log([E + p_z]/[E - p_z])$. The comparison of the width of the dN_{ch}/dy at different collision energies provides an insight into the constraints on the overall production mechanism of charged particles.

2. Experimental setup

A detailed description of ALICE and its performance can be found elsewhere [9,10]. In the following, we briefly describe the detectors relevant to this analysis.

^{*} E-mail address: alice-publications@cern.ch.

The Silicon Pixel Detector (SPD), the innermost part of the Inner Tracking System (ITS), consists of two cylindrical layers of hybrid silicon pixel assemblies covering $|\eta| < 2$ and $|\eta| < 1.4$ for the inner and outer layers, respectively. Combinations of hits on each of the two layers consistent with tracks originating from the interaction point form *tracklets*.

The Forward Multiplicity Detector (FMD) is a silicon strip detector which, records the energy deposited by particles traversing the it. The detector covers the pseudorapidity regions $-3.5 < \eta < -1.8$ and $1.8 < \eta < 5$, and has almost full coverage in azimuth (ϕ), and high granularity in the radial (η) direction.

The third detector system used in this analysis is the V0. It consists of two sub-detectors: V0-A and V0-C covering the pseudorapidity regions $2.8 < \eta < 5.1$ and $-3.7 < \eta < -1.7$, respectively, each made up of scintillator tiles with a timing resolution < 1 ns. The fast signals from either of V0-A or V0-C are combined in a programmable logic to form a trigger signal and to reject background events. Furthermore, the combined pulse height signal of both sub-detectors forms the basis for the classification of events into different centrality classes [11].

The Zero-Degree Calorimeter (ZDC) measures the energy of spectator (non-interacting) nucleons with two components: one measures protons and the other measures neutrons. The ZDC is located at about 112.5 m from the interaction point on both sides of the experiment [9]. The ZDC also provides timing information used to select collisions in the off-line data processing.

3. Data sample and analysis method

The results presented here are based on data collected by ALICE in 2015 during the Pb–Pb collision run of the LHC at $\sqrt{s_{NN}} = 5.02$ TeV. About 100 000 events with a minimum bias trigger requirement [12] were analysed in the centrality range from 0% to 90%. The minimum bias trigger for Pb–Pb collisions in ALICE, which defines the so-called visible cross-section, is defined as a coincidence between the A ($z > 0$) and C ($z < 0$) sides of the V0 detector.

The standard ALICE event selection [13] and centrality estimator based on the V0–amplitude [11] are used in this analysis. The event selection consists of: exclusion of background events using the timing information from the ZDC and V0 detectors; verification of the trigger conditions; and a reconstructed position of the collision. As discussed elsewhere [11], the 90–100% centrality class has substantial contributions from QED processes and is therefore not included in the results presented here.

The measurement of the charged-particle pseudorapidity density at mid-rapidity ($|\eta| < 2$) is obtained from a tracklet analysis using the two layers of the SPD. The analysis method used is identical to what has previously been presented [12,14,15]. Note that no attempt is made to correct for known deficiencies, such as deviations in the number of strange particles or transverse momentum (p_T) distributions compared to experimental measurements [11,16,17], in the event generators used to obtain the corrections from simulations (e.g., HIJING). It is found, through simulation studies, that tracklet reconstruction first and foremost depends on the local hit density and only weakly on particle mix and transverse momentum. For example, the deficit of strange particles in the event generator effects the result by less than 2%. Since the event generators generally, after detector simulation, produce a local hit density that is consistent with what is observed in data, we observe a correspondence between the tracklet samples of both simulations and data. On the other hand, changing the number of tracklets corresponding to strange particles a posteriori to match the measured relative yields dramatically biases the simulated tracklet sample away from the measured, thus entailing systematic uncertainties that are beyond the effect of the known event generator deficiencies, and

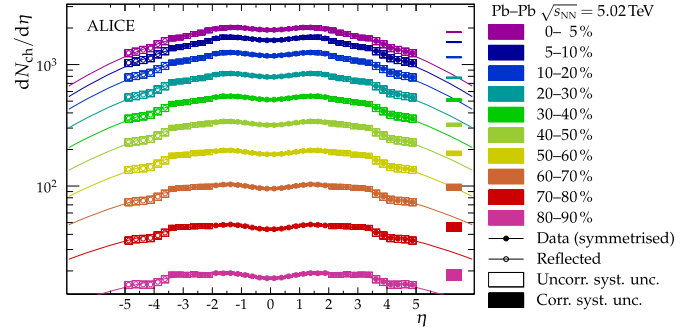


Fig. 1. [Colour online.] Charged-particle pseudorapidity density for ten centrality classes over a broad η range in Pb–Pb collisions at $\sqrt{s_{NN}} = 5.02$ TeV. Boxes around the points reflect the total uncorrelated systematic uncertainties, while the filled squares on the right reflect the correlated systematic uncertainty (evaluated at $\eta = 0$). Statistical errors are generally insignificant and smaller than the markers. Also shown is the reflection of the $3.5 < \eta < 5$ values around $\eta = 0$ (open circles). The line corresponds to fits of the difference between two Gaussians centred at $\eta = 0$ (f_{GG}) [7] to the data.

as such do not improve the accuracy of the measurements. Instead, variations on the event generators are used to estimate the systematic uncertainties as detailed elsewhere [12,14,15].

In the forward regions ($-3.5 < \eta < -1.8$ and $1.8 < \eta < 5$), the measurement is provided by the analysis of the deposited energy signal in the FMD. The analysis method used is identical to what has previously been presented [7,14]: a statistical approach to calculate the inclusive number of charged particles; and a data-driven correction – derived from previous satellite-main collisions – to remove the large background from secondary particles.

4. Systematic uncertainties

For the measurements at mid-rapidity the sources and dependencies of the systematic uncertainties are detailed elsewhere [7,12,15]. The magnitude of the systematic uncertainties is unchanged with respect to previous results, and amounts to 2.6% at $\eta = 0$ and 2.9% at $\eta = 2$, most of which is correlated over $|\eta| < 2$, and largely independent of centrality.

The systematic uncertainty on the forward analysis is evaluated using the same technique as for previous results [7]. We find that the uncertainty is uncorrelated across η and that it amounts to 6.9% for $\eta > 3.5$ and 6.4% elsewhere within the forward regions.

The systematic uncertainty on $dN_{ch}/d\eta$ due to the centrality class definition is estimated as 0.6% for the most central and 9.5% for the most peripheral class [15]. The uncertainty is estimated by using alternative centrality definitions based on SPD hit multiplicities and by varying the fraction of the visible hadronic cross-section. The 80–90% centrality class has some residual contamination from electromagnetic processes detailed elsewhere [11], which gives rise to a 4% additional systematic uncertainty on the measurements.

In summary, the total systematic uncertainty varies from 2.6% at mid-rapidity in the most central collisions to 12.4% at the very forward rapidities for the most peripheral collisions.

5. Results

Fig. 1 presents the charged-particle pseudorapidity density as a function of pseudorapidity for ten centrality classes. The measurements from the SPD and FMD are combined in regions of overlap ($1.8 < |\eta| < 2$) between the two detectors by taking the weighted average using the non-shared uncertainties as weights. Finally, based on the symmetry of the collision system, the result is symmetrized around $\eta = 0$, and extended into the non-measured

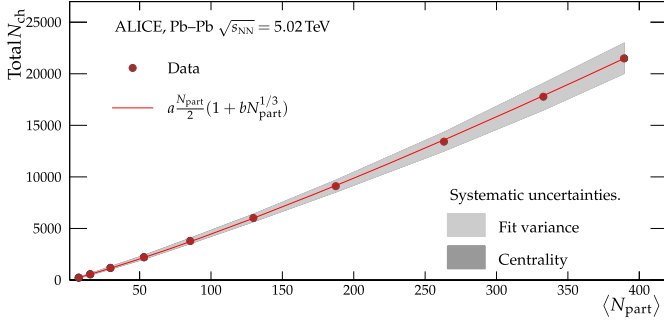


Fig. 2. [Colour online.] Total number of charged particles as a function of the mean number of participating nucleons [11]. The total charged-particle multiplicity is given as the integral over $dN_{\text{ch}}/d\eta$ over the measured region ($-3.5 < \eta < 5$) and extrapolations from fitted functions in the unmeasured regions. The contribution from unmeasured η regions amounts to $\approx 30\%$ of the total number of charged particles. The uncertainty on the extrapolation to the unmeasured pseudorapidity region is smaller than the size of the markers. The contribution to the systematic uncertainties from the centrality determination and electromagnetic processes are vanishing compared to the contribution from the largest differences between the fitted functions. A function inspired by factorisation [18] is fitted to the data, and the best fit yields $a = 51.5 \pm 7.3$, $b = 0.16 \pm 0.05$.

region $-5 < \eta < -3.5$ by reflecting the $3.5 < \eta < 5$ values around $\eta = 0$. Complementing result previously reported at mid-rapidity [15], we find $dN_{\text{ch}}/d\eta|_{|\eta|<0.5} = 17.52 \pm 0.05(\text{stat}) \pm 1.84(\text{sys})$ and $N_{\text{part}} = 7.3 \pm 0.1$ in the 80–90% centrality class.

The measured distributions are fitted with four functions f_{GG} , f_{P} , f_{T} , and f_{B} [7], which are the difference of two Gaussian distributions centred at $\eta = 0$; a parametrisation proposed by PHOBOS [18]; a trapezoidal form; and a plateau connected to Gaussian tails, respectively. To extract the total number of charged particles, we calculate the integral and uncertainty from the data in the measured region and use the integrals of the fitted functions in the unmeasured regions up to the beam rapidity $\pm y_{\text{beam}} = \pm 8.6$. As for the previous measurements at $\sqrt{s_{\text{NN}}} = 5.02$ TeV, the central value in the unmeasured regions ($-8.6 < \eta < -3.5$ and $5 < \eta < 8.6$) is taken from the fit of the function f_{T} , while the uncertainty is evaluated as the largest difference between the fitted functions scaled by $1/\sqrt{3}$ [7,14]. The total charged-particle multiplicity is shown in Fig. 2 versus the mean number of participating nucleons ($\langle N_{\text{part}} \rangle$) estimated from a Glauber calculation [11,15]. After removing correlated systematic uncertainties, we observe an increase in the total number of charged particles ($27 \pm 4\%$) with respect to the measurements at $\sqrt{s_{\text{NN}}} = 2.76$ TeV [7] for all centrality classes. The line shown in Fig. 2 corresponds to a fit of a function inspired by factorisation [18]. The function illustrates scaling by number of participant pairs, with a small perturbation proportional to the cubic root of the number of participants. As the number of nucleon–nucleon collisions (N_{coll}) scales roughly like the square of the number of participants $N_{\text{coll}} \approx N_{\text{part}}^2$ [19], we see no indication of scaling by number of nucleon–nucleon collisions. The observed total N_{ch} dependence on $\langle N_{\text{part}} \rangle$ provides no evidence of any significant increase in the number of hard scatterings between the participating nucleons and partons.

In Fig. 3, we compare the charged-particle pseudorapidity density for the 0–5% most central collisions to three models: HIJING [20]; EPOS-LHC [21]; and KLN [22,23], also for the 0–5% most central, except for KLN which is shown for the 0–6% centrality class. Two versions of HIJING are used: version 1.383, with jet quenching disabled, shadowing enabled, and a hard p_{T} cut-off of 2.3 GeV; and the newer version 2.1 [24]. Both are two-component models with a soft and hard sector defined by a p_{T} cut-off separating the two. In the 2.1 implementation, HIJING uses an up-graded parametrisation of the nuclear parton distribution func-

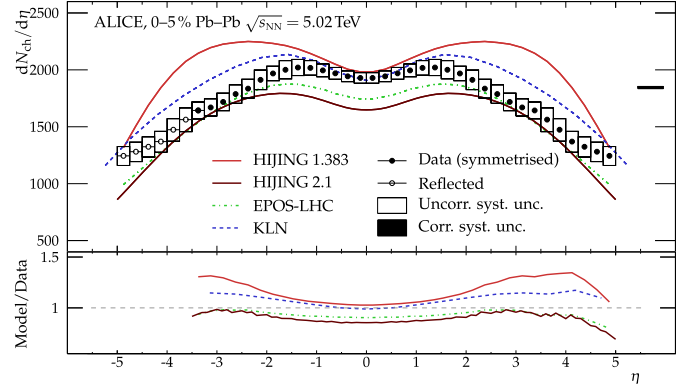


Fig. 3. [Colour online.] Comparison of $dN_{\text{ch}}/d\eta$ in the 0–5% (0–6% for KLN) most central collisions of two versions of HIJING, KLN, and EPOS-LHC model calculations to the measured distribution.

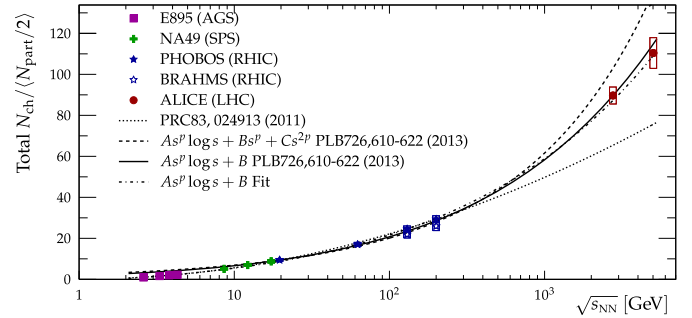


Fig. 4. [Colour online.] Total number of charged particles as a function of $\sqrt{s_{\text{NN}}}$ for the most central collisions at AGS (0–5% Au–Au) [25,26], SPS (0–5% Pb–Pb) [27,28], RHIC (0–5% and 0–6% Au–Au) [18,29,30], and LHC (0–5% Pb–Pb) [14]. The dotted, dashed, and full lines are extrapolations from fits to lower energy results [14], while the dash-dotted line is a fit over all energies, including $\sqrt{s_{\text{NN}}} = 5.02$ TeV.

tions. This results in a larger cross section for soft processes and a smaller cross section for jet production. The KLN model is based on Colour-Glass-Condensate initial conditions, while EPOS-LHC uses so-called parton-ladders which hadronise in a medium. While none of the three models describe the measured charged-particle pseudorapidity density over the full pseudorapidity range, we observe some differences: HIJING 1.383 over-predicts the charged-particle production especially away from $\eta \approx 0$; EPOS-LHC and HIJING 2.1 consistently under-predict the charge-particle production; whereas KLN, EPOS-LHC, and HIJING 2.1 give a shape reasonably close to the observed distribution. Not shown in Fig. 3, for both HIJING 1.383 and EPOS-LHC, these observations hold over all centrality classes i.e., HIJING 1.383 consistently produces far too many particles away from mid-rapidity and EPOS-LHC consistently under-predicts the charged-particle yield over the full η range. These trends become increasingly more pronounced for more peripheral collisions.

Fig. 4 shows the total number of charged particles produced in the most central heavy-ion collisions as a function of the collision energy, ranging from $\sqrt{s_{\text{NN}}} = 2.6$ GeV to 5.02 TeV [14]. The dotted, dashed, and full-drawn lines in the figure represent extrapolations from lower energy results to the current top LHC energy of $\sqrt{s_{\text{NN}}} = 5.02$ TeV. None of these predictions fully describe the data. A refit of the simple model of a logarithmic-dampened power-law in the square collision energy (s) including from the lowest to the highest energy results, shown as the dash-dotted line, does accurately describe the total number of charged particles at all available energies.

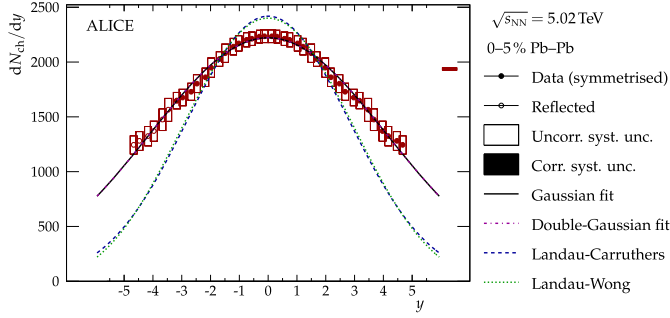


Fig. 5. [Colour online.] Estimate of dN_{ch}/dy in the most central (0–5%) Pb–Pb collisions at $\sqrt{s_{\text{NN}}} = 5.02$ TeV. Also shown are the Landau–Wong [31], Landau–Carruthers [32], Gaussian, and double-Gaussian distributions.

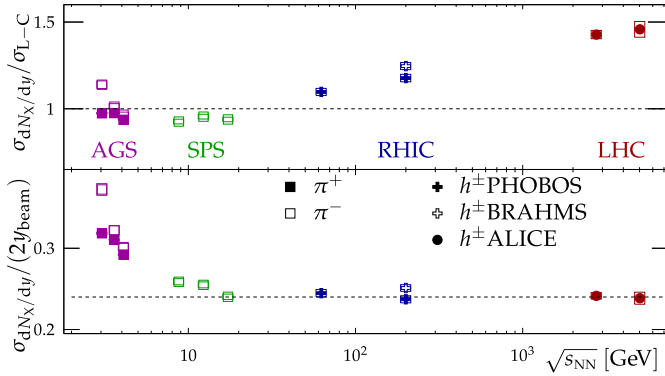


Fig. 6. [Colour online.] Scaling behaviour as a function $\sqrt{s_{\text{NN}}}$ of the width of the charged-particle or -pion rapidity-density distribution with respect to the Landau–Carruthers width (top) and rapidity range (bottom). Charged-pion points from AGS and SPS are adapted from the literature [33], while the PHOBOS (filled crosses) [34] and BRAHMS (open crosses) [30] charged-hadron points are translated from the corresponding $dN_{\text{ch}}/d\eta$ results.

We can calculate the Jacobian transform from η to rapidity y by assuming the same transverse momentum distribution of (anti-)protons, and charged kaons and pions, and the same particle ratios in Pb–Pb collisions at $\sqrt{s_{\text{NN}}} = 5.02$ TeV as in $\sqrt{s_{\text{NN}}} = 2.76$ TeV. The result is presented in Fig. 5 for the 0–5% most central collisions. The effect on the Jacobian from the change of p_T spectra and particle ratios when increasing the collision energy by almost a factor two is evaluated using the EPOS–LHC model [21]. It is found, that the effect is at most 3% on both dN_{ch}/dy and y – much smaller than the systematic uncertainty and η resolution of the analysis. Fig. 5 also shows the expected charged-particle rapidity densities from the Landau–Carruthers [32] and Landau–Wong [31] models, both assuming Landau hydrodynamics i.e., based on a reaction scenario with full stopping of the reaction partners and a subsequent thermodynamic evolution. The measurements, however, are seen to be consistent with a Gaussian distribution with a width of 4.12 ± 0.10 , much wider than the width expected from the two models. A best parameter fit of the sum of two Gaussian distributions with means symmetric around $y = 0$, is indistinguishable from the single Gaussian case.

In the top part of Fig. 6 we compare the widths of the charged-particle or -pion rapidity density distribution extracted from measurements to the expected width $\sigma_{\text{L-C}}^2 = \log(\sqrt{s_{\text{NN}}}/2m_p)$ from Landau–Carruthers, where m_p is the proton mass, at collision energies ranging from 2.6 GeV up to 5.02 TeV. An increase of $\approx 7\%$ of $\sigma_{dN_{\text{ch}}/dy}/\sigma_{\text{L-C}}$ is seen from the $\sqrt{s_{\text{NN}}} = 2.76$ TeV ALICE measurements [14]. The full evolution is consistent with an almost linear rise as a function of $\log \sqrt{s_{\text{NN}}}$ from the top SPS energy at $\sqrt{s_{\text{NN}}} = 17.3$ GeV. It can be shown [35] that the width of

the rapidity-density distribution in Landau hydrodynamics scales as $\sigma_{dN_{\text{ch}}/dy} \propto 1/(1-c_s^2)$, where c_s is the speed of sound in the matter. The lifetime of the system scales inversely with c_s , and given that the measured width is larger than the predicted by Landau hydrodynamics, it is an indication that, given the considerations above, the lifetime is shorter than suggested.

In the bottom part of Fig. 6 we compare the width of the dN_{ch}/dy distribution to the available rapidity range ($2y_{\text{beam}}$). We observe no dependence of this ratio from $\sqrt{s_{\text{NN}}} = 17.3$ GeV and upward, indicating that the available phase-space constrains the width of that distribution. The charged-hadron measurements at RHIC (crosses) from the BRAHMS [30] and PHOBOS [34] measurements of $dN_{\text{ch}}/d\eta$ are converted to dN_{ch}/dy using the same method as applied to the ALICE data. Previously, charged-pion measurements from BRAHMS have been reported [33]. These data are not included because a re-evaluation using RHIC Run-4 Au–Au data has not been finalised [36].

From the observed s^p scaling of the charged-particle pseudorapidity density at mid-rapidity [15] we expect a 20% increase over $\sqrt{s_{\text{NN}}} = 2.76$ TeV in the level of $dN_{\text{ch}}/d\eta|_{|\eta|<0.5}$ and from the extracted width of dN_{ch}/dy we observe an additional 7%, consistent with the increase of 27% over $\sqrt{s_{\text{NN}}} = 2.76$ TeV in the total number of charged particles produced in $\sqrt{s_{\text{NN}}} = 5.02$ TeV collisions.

6. Conclusions

The charged-particle pseudorapidity density is measured in Pb–Pb collisions at $\sqrt{s_{\text{NN}}} = 5.02$ TeV over the pseudorapidity range $-3.5 < \eta < 5$. The total number of charged particles produced is determined owing to the large pseudorapidity acceptance of ALICE. The latter increases by two orders of magnitude from the most peripheral to the most central collisions and scales approximately with the number of participating nucleons. The increase in the total number of charged particles relative to $\sqrt{s_{\text{NN}}} = 2.76$ TeV is estimated to be $(27 \pm 4)\%$. The charged-particle rapidity density for the most central collisions is extracted, and the width of that distribution is compared to predictions from the Landau–Carruthers and Landau–Wong hydrodynamic models. It is found that the measured charged-particle rapidity density becomes increasingly wider as a function of collision energy than predicted by Landau hydrodynamics. The width of the charged-particle rapidity density is seen to scale with the beam rapidity, which implies that the available phase space determines the longitudinal extend of the charged-particle production. The phase space dominance starts at the top SPS energy and persist for two orders of magnitude up to the top LHC energy.

Acknowledgements

The ALICE Collaboration would like to thank all its engineers and technicians for their invaluable contributions to the construction of the experiment and the CERN accelerator teams for the outstanding performance of the LHC complex. The ALICE Collaboration gratefully acknowledges the resources and support provided by all Grid centres and the Worldwide LHC Computing Grid (WLCG) collaboration. The ALICE Collaboration acknowledges the following funding agencies for their support in building and running the ALICE detector: A.I. Alikhanyan National Science Laboratory (Yerevan Physics Institute) Foundation (ANS), State Committee of Science and World Federation of Scientists (WFS), Armenia; Austrian Academy of Sciences and Nationalstiftung für Forschung, Technologie und Entwicklung, Austria; Conselho Nacional de Desenvolvimento Científico e Tecnológico (CNPq), Universidade Federal do Rio Grande do Sul (UFRGS), Financiadora de Estudos e Projetos (Finep) and Fundação de Amparo à Pesquisa do Estado

de São Paulo (FAPESP), Brazil; Ministry of Science & Technology of China (MSTC), National Natural Science Foundation of China (NSFC) and Ministry of Education of China (MOEC), China; Ministry of Science, Education and Sport and Croatian Science Foundation, Croatia; Ministry of Education, Youth and Sports of the Czech Republic, Czech Republic; The Danish Council for Independent Research–Natural Sciences, the Carlsberg Foundation and Danish National Research Foundation (DNRF), Denmark; Helsinki Institute of Physics (HIP), Finland; Commissariat à l’Énergie Atomique (CEA) and Institut National de Physique Nucléaire et de Physique des Particules (IN2P3) and Centre National de la Recherche Scientifique (CNRS), France; Bundesministerium für Bildung, Wissenschaft, Forschung und Technologie (BMBF) and GSI Helmholtzzentrum für Schwerionenforschung GmbH, Germany; Ministry of Education, Research and Religious Affairs, Greece; National Research, Development and Innovation Office, Hungary; Department of Atomic Energy, Government of India (DAE) and Council of Scientific and Industrial Research (CSIR), New Delhi, India; Indonesian Institute of Science, Indonesia; Centro Fermi - Museo Storico della Fisica e Centro Studi e Ricerche Enrico Fermi and Istituto Nazionale di Fisica Nucleare (INFN), Italy; Institute for Innovative Science and Technology, Nagasaki Institute of Applied Science (IIST), Japan Society for the Promotion of Science (JSPS) KAKENHI and Japanese Ministry of Education, Culture, Sports, Science and Technology (MEXT), Japan; Consejo Nacional de Ciencia y Tecnología (CONACYT), through Fondo de Cooperación Internacional en Ciencia y Tecnología (FONCICT) and Dirección General de Asuntos del Personal Académico (DGAPA), Mexico; Nationaal instituut voor subatomaire fysica (Nikhef), Netherlands; The Research Council of Norway, Norway; Commission on Science and Technology for Sustainable Development in the South (COMSATS), Pakistan; Pontificia Universidad Católica del Perú, Peru; Ministry of Science and Higher Education and National Science Centre, Poland; Korea Institute of Science and Technology Information and National Research Foundation of Korea (NRF), Republic of Korea; Ministry of Education and Scientific Research, Institute of Atomic Physics and Romanian National Agency for Science, Technology and Innovation, Romania; Joint Institute for Nuclear Research (JINR), Ministry of Education and Science of the Russian Federation and National Research Centre Kurchatov Institute, Russia; Ministry of Education, Science, Research and Sport of the Slovak Republic, Slovakia; National Research Foundation of South Africa, South Africa; Centro de Aplicaciones Tecnológicas y Desarrollo Nuclear (CEADEN), Cubaenergía, Cuba, Ministerio de Ciencia e Innovación and Centro de Investigaciones Energéticas, Medioambientales y Tecnológicas (CIEMAT), Spain; Swedish Research Council (VR) and Knut & Alice Wallenberg Foundation (KAW), Sweden; European Organization for Nuclear Research, Switzerland; National Science and Technology Development Agency (NSDTA), Suranaree University of Technology (SUT) and Office of the Higher Education Commission under NRU project of Thailand, Thailand; Turkish Atomic Energy Agency (TAEK), Turkey; National Academy of Sciences of Ukraine, Ukraine; Science and Technology Facilities Council (STFC), United Kingdom; National Science Foundation of the United States of America (NSF) and United States Department of Energy, Office of Nuclear Physics (DOE NP), United States of America.

References

- [1] BRAHMS Collaboration, I. Arsene, et al., Quark gluon plasma and color glass condensate at RHIC? The Perspective from the BRAHMS experiment, *Nucl. Phys. A* 757 (2005) 1–27, arXiv:nucl-ex/0410020.
- [2] PHOBOS Collaboration, B.B. Back, et al., The PHOBOS perspective on discoveries at RHIC, *Nucl. Phys. A* 757 (2005) 28–101, arXiv:nucl-ex/0410022.
- [3] STAR Collaboration, J. Adams, et al., Experimental and theoretical challenges in the search for the quark gluon plasma: the STAR Collaboration’s critical assessment of the evidence from RHIC collisions, *Nucl. Phys. A* 757 (2005) 102–183, arXiv:nucl-ex/0501009.
- [4] PHENIX Collaboration, K. Adcox, et al., Formation of dense partonic matter in relativistic nucleus–nucleus collisions at RHIC: experimental evaluation by the PHENIX collaboration, *Nucl. Phys. A* 757 (2005) 184–283, arXiv:nucl-ex/0410003.
- [5] J.L. Nagle, The letter S (and the sQGP), *Eur. Phys. J. C* 49 (2007) 275–279, arXiv:nucl-th/0608070.
- [6] N. Armesto, Predictions for the heavy-ion programme at the Large Hadron Collider, in: R.C. Hwa, X.-N. Wang (Eds.), *Quark–Gluon Plasma 4*, World Scientific, 2012, pp. 375–437, arXiv:0903.1330.
- [7] ALICE Collaboration, J. Adam, et al., Centrality evolution of the charged-particle pseudorapidity density over a broad pseudorapidity range in Pb–Pb collisions at $\sqrt{s_{NN}} = 2.76$ TeV, *Phys. Lett. B* 754 (2016) 373–385, arXiv:1509.07299 [nucl-ex].
- [8] ALICE Collaboration, J. Adam, et al., The ALICE definition of primary particles, ALICE-PUBLIC-2017-005, <https://cds.cern.ch/record/2270008>, Jun 2017.
- [9] ALICE Collaboration, K. Aamodt, et al., The ALICE experiment at the CERN LHC, *J. Instrum.* 3 (2008) S08002.
- [10] ALICE Collaboration, B. Abelev, et al., Performance of the ALICE experiment at the CERN LHC, *Int. J. Mod. Phys. A* 29 (2014) 1430044, arXiv:1402.4476 [nucl-ex].
- [11] ALICE Collaboration, B. Abelev, et al., Centrality determination of Pb–Pb collisions at $\sqrt{s_{NN}} = 2.76$ TeV with ALICE, *Phys. Rev. C* 88 (2013) 044909, arXiv:1301.4361 [nucl-ex].
- [12] ALICE Collaboration, K. Aamodt, et al., Centrality dependence of the charged-particle multiplicity density at mid-rapidity in Pb–Pb collisions at $\sqrt{s_{NN}} = 2.76$ TeV, *Phys. Rev. Lett.* 106 (2011) 032301, arXiv:1012.1657 [nucl-ex].
- [13] ALICE Collaboration, K. Aamodt, et al., Charged-particle multiplicity density at mid-rapidity in central Pb–Pb collisions at $\sqrt{s_{NN}} = 2.76$ TeV, *Phys. Rev. Lett.* 105 (2010) 252301, arXiv:1011.3916 [nucl-ex].
- [14] ALICE Collaboration, E. Abbas, et al., Centrality dependence of the pseudorapidity density distribution for charged particles in Pb–Pb collisions at $\sqrt{s_{NN}} = 2.76$ TeV, *Phys. Lett. B* 726 (2013) 610–622, arXiv:1304.0347 [nucl-ex].
- [15] ALICE Collaboration, J. Adam, et al., Centrality dependence of the charged-particle multiplicity density at midrapidity in Pb–Pb collisions at $\sqrt{s_{NN}} = 5.02$ TeV, *Phys. Rev. Lett.* 116 (2016) 222302, arXiv:1512.06104 [nucl-ex].
- [16] ALICE Collaboration, B.B. Abelev, et al., Centrality, rapidity and transverse momentum dependence of J/ψ suppression in Pb–Pb collisions at $\sqrt{s_{NN}} = 2.76$ TeV, *Phys. Lett. B* 734 (2014) 314–327, arXiv:1311.0214 [nucl-ex].
- [17] ALICE Collaboration, B.B. Abelev, et al., K_S^0 and Λ production in Pb–Pb collisions at $\sqrt{s_{NN}} = 2.76$ TeV, *Phys. Rev. Lett.* 111 (2013) 222301, arXiv:1307.5530 [nucl-ex].
- [18] PHOBOS Collaboration, B. Alver, et al., Charged-particle multiplicity and pseudorapidity distributions measured with the PHOBOS detector in Au+Au, Cu+Cu, d+Au, p+p collisions at ultrarelativistic energies, *Phys. Rev. C* 83 (2011) 024913, arXiv:1011.1940 [nucl-ex].
- [19] ALICE Collaboration, J. Adam, et al., Centrality dependence of the charged-particle multiplicity density at midrapidity in Pb–Pb collisions at $\sqrt{s_{NN}} = 5.02$ TeV, <https://cds.cern.ch/record/2118084>.
- [20] X.-N. Wang, M. Gyulassy, HIJING: a Monte Carlo model for multiple jet production in pp, pA and AA collisions, *Phys. Rev. D* 44 (1991) 3501–3516.
- [21] T. Pierog, I. Karpenko, J.M. Katzy, E. Yatsenko, K. Werner, EPOS LHC: test of collective hadronization with data measured at the CERN Large Hadron Collider, *Phys. Rev. C* 92 (2015) 034906, arXiv:1306.0121 [hep-ph].
- [22] D. Kharzeev, E. Levin, M. Nardi, Color glass condensate at the LHC: hadron multiplicities in pp, pA and AA collisions, *Nucl. Phys. A* 747 (2005) 609–629, arXiv:hep-ph/0408050.
- [23] A. Dumitru, D.E. Kharzeev, E.M. Levin, Y. Nara, Gluon saturation in pA collisions at the LHC: KLN model predictions for hadron multiplicities, *Phys. Rev. C* 85 (2012) 044920, arXiv:1111.3031 [hep-ph].
- [24] W.-T. Deng, X.-N. Wang, R. Xu, Hadron production in p+p, p+Pb, and Pb+Pb collisions with the HIJING 2.0 model at energies available at the CERN Large Hadron Collider, *Phys. Rev. C* 83 (2011) 014915, arXiv:1008.1841 [hep-ph].
- [25] E-895 Collaboration, J.L. Klay, et al., Charged pion production in 2A to 8A GeV central Au + Au Collisions, *Phys. Rev. C* 68 (2003) 054905, arXiv:nucl-ex/0306033.
- [26] E-802 Collaboration, L. Ahle, et al., Particle production at high baryon density in central Au+Au reactions at 11.6A GeV/c, *Phys. Rev. C* 57 (1998) R466–R470.
- [27] NA49 Collaboration, S.V. Afanasiev, et al., Energy dependence of pion and kaon production in central Pb+Pb collisions, *Phys. Rev. C* 66 (2002) 054902, arXiv:nucl-ex/0205002.
- [28] NA50 Collaboration, M.C. Abreu, et al., Scaling of charged particle multiplicity in Pb–Pb collisions at SPS energies, *Phys. Lett. B* 530 (2002) 43–55.
- [29] BRAHMS Collaboration, I.G. Bearden, et al., Charged particle densities from Au+Au collisions at $\sqrt{s_{NN}} = 130$ GeV, *Phys. Lett. B* 523 (2001) 227–233, arXiv:nucl-ex/0108016.
- [30] BRAHMS Collaboration, I.G. Bearden, et al., Pseudorapidity distributions of charged particles from Au+Au collisions at the maximum RHIC energy, *Phys. Rev. Lett.* 88 (2002) 202301, arXiv:nucl-ex/0112001.

- [31] C.-Y. Wong, Landau hydrodynamics revisited, *Phys. Rev. C* 78 (2008) 054902, arXiv:0808.1294 [hep-ph].
- [32] P. Carruthers, M. Duong-Van, New scaling law based on the hydrodynamical model of particle production, *Phys. Lett. B* 41 (1972) 597–601.
- [33] BRAHMS Collaboration, I.G. Bearden, et al., Charged meson rapidity distributions in central Au+Au collisions at $\sqrt{s_{NN}} = 200$ GeV, *Phys. Rev. Lett.* 94 (2005) 162301, arXiv:nucl-ex/0403050.
- [34] PHOBOS Collaboration, B.B. Back, et al., The significance of the fragmentation region in ultrarelativistic heavy ion collisions, *Phys. Rev. Lett.* 91 (2003) 052303, arXiv:nucl-ex/0210015.
- [35] B. Mohanty, J.-e. Alam, Velocity of sound in relativistic heavy ion collisions, *Phys. Rev. C* 68 (2003) 064903, arXiv:nucl-th/0301086.
- [36] BRAHMS Collaboration, F. Videbæk, Overview and recent results from BRAHMS, *Nucl. Phys. A* 830 (2009) 43C–50C, arXiv:0907.4742 [nucl-ex].

ALICE Collaboration

J. Adam³⁸, D. Adamová⁸⁶, M.M. Aggarwal⁹⁰, G. Aglieri Rinella³⁴, M. Agnello^{30,112}, N. Agrawal⁴⁷, Z. Ahammed¹³⁷, S. Ahmad¹⁷, S.U. Ahn⁶⁹, S. Aiola¹⁴¹, A. Akindinov⁵⁴, S.N. Alam¹³⁷, D.S.D. Albuquerque¹²³, D. Aleksandrov⁸², B. Alessandro¹¹², D. Alexandre¹⁰³, R. Alfaro Molina⁶⁴, A. Alici^{12,106}, A. Alkin³, J. Alme^{21,36}, T. Alt⁴¹, S. Altinpinar²¹, I. Altsybeev¹³⁶, C. Alves Garcia Prado¹²², M. An⁷, C. Andrei⁸⁰, H.A. Andrews¹⁰³, A. Andronic⁹⁹, V. Anguelov⁹⁵, C. Anson⁸⁹, T. Antičić¹⁰⁰, F. Antinori¹⁰⁹, P. Antonioli¹⁰⁶, R. Anwar¹²⁵, L. Aphecetche¹¹⁵, H. Appelshäuser⁶⁰, S. Arcelli²⁶, R. Arnaldi¹¹², O.W. Arnold^{96,35}, I.C. Arsene²⁰, M. Arslanodok⁶⁰, B. Audurier¹¹⁵, A. Augustinus³⁴, R. Auerbeck⁹⁹, M.D. Azmi¹⁷, A. Badalà¹⁰⁸, Y.W. Baek⁶⁸, S. Bagnasco¹¹², R. Bailhache⁶⁰, R. Bala⁹², A. Baldissieri⁶⁵, R.C. Baral⁵⁷, A.M. Barbano²⁵, R. Barbera²⁷, F. Barile³², L. Barioglio²⁵, G.G. Barnaföldi¹⁴⁰, L.S. Barnby^{103,34}, V. Barret⁷¹, P. Bartalini⁷, K. Barth³⁴, J. Bartke^{119,i}, E. Bartsch⁶⁰, M. Basile²⁶, N. Bastid⁷¹, S. Basu¹³⁷, B. Bathen⁶¹, G. Batigne¹¹⁵, A. Batista Camejo⁷¹, B. Batyunya⁶⁷, P.C. Batzing²⁰, I.G. Bearden⁸³, H. Beck⁹⁵, C. Bedda³⁰, N.K. Behera⁵⁰, I. Belikov¹³⁴, F. Bellini²⁶, H. Bello Martinez², R. Bellwied¹²⁵, L.G.E. Beltran¹²¹, V. Belyaev⁷⁶, G. Bencedi¹⁴⁰, S. Beole²⁵, A. Bercuci⁸⁰, Y. Berdnikov⁸⁸, D. Berenyi¹⁴⁰, R.A. Bertens^{53,128}, D. Berzano³⁴, L. Betev³⁴, A. Bhasin⁹², I.R. Bhat⁹², A.K. Bhati⁹⁰, B. Bhattacharjee⁴³, J. Bhom¹¹⁹, L. Bianchi¹²⁵, N. Bianchi⁷³, C. Bianchin¹³⁹, J. Bielčik³⁸, J. Bielčíková⁸⁶, A. Bilandzic^{35,96}, G. Biro¹⁴⁰, R. Biswas⁴, S. Biswas⁴, J.T. Blair¹²⁰, D. Blau⁸², C. Blume⁶⁰, F. Bock^{75,95}, A. Bogdanov⁷⁶, L. Boldizsár¹⁴⁰, M. Bombara³⁹, M. Bonora³⁴, J. Book⁶⁰, H. Borel⁶⁵, A. Borissov⁹⁸, M. Borri¹²⁷, E. Botta²⁵, C. Bourjau⁸³, P. Braun-Munzinger⁹⁹, M. Bregant¹²², T.A. Broker⁶⁰, T.A. Browning⁹⁷, M. Broz³⁸, E.J. Brucken⁴⁵, E. Bruna¹¹², G.E. Bruno³², D. Budnikov¹⁰¹, H. Buesching⁶⁰, S. Bufalino^{30,25}, P. Buhler¹¹⁴, S.A.I. Buitron⁶², P. Buncic³⁴, O. Busch¹³¹, Z. Buthelezi⁶⁶, J.B. Butt¹⁵, J.T. Buxton¹⁸, J. Cabala¹¹⁷, D. Caffarri³⁴, H. Caines¹⁴¹, A. Caliva⁵³, E. Calvo Villar¹⁰⁴, P. Camerini²⁴, A.A. Capon¹¹⁴, F. Carena³⁴, W. Carena³⁴, F. Carnesecchi^{26,12}, J. Castillo Castellanos⁶⁵, A.J. Castro¹²⁸, E.A.R. Casula^{23,107}, C. Ceballos Sanchez⁹, P. Cerello¹¹², J. Cercala¹¹⁷, B. Chang¹²⁶, S. Chapeland³⁴, M. Chartier¹²⁷, J.L. Charvet⁶⁵, S. Chattopadhyay¹³⁷, S. Chattopadhyay¹⁰², A. Chauvin^{96,35}, M. Cherney⁸⁹, C. Cheshkov¹³³, B. Cheynis¹³³, V. Chibante Barroso³⁴, D.D. Chinellato¹²³, S. Cho⁵⁰, P. Chochula³⁴, K. Choi⁹⁸, M. Chojnacki⁸³, S. Choudhury¹³⁷, P. Christakoglou⁸⁴, C.H. Christensen⁸³, P. Christiansen³³, T. Chujo¹³¹, S.U. Chung⁹⁸, C. Cicalo¹⁰⁷, L. Cifarelli^{12,26}, F. Cindolo¹⁰⁶, J. Cleymans⁹¹, F. Colamaria³², D. Colella^{55,34}, A. Collu⁷⁵, M. Colocci²⁶, G. Conesa Balbastre⁷², Z. Conesa del Valle⁵¹, M.E. Connors^{141,ii}, J.G. Contreras³⁸, T.M. Cormier⁸⁷, Y. Corrales Morales¹¹², I. Cortés Maldonado², P. Cortese³¹, M.R. Cosentino^{122,124}, F. Costa³⁴, J. Crkovská⁵¹, P. Crochet⁷¹, R. Cruz Albino¹¹, E. Cuautle⁶², L. Cunqueiro⁶¹, T. Dahms^{35,96}, A. Dainese¹⁰⁹, M.C. Danisch⁹⁵, A. Danu⁵⁸, D. Das¹⁰², I. Das¹⁰², S. Das⁴, A. Dash⁸¹, S. Dash⁴⁷, S. De^{48,122}, A. De Caro²⁹, G. de Cataldo¹⁰⁵, C. de Conti¹²², J. de Cuveland⁴¹, A. De Falco²³, D. De Gruttola^{12,29}, N. De Marco¹¹², S. De Pasquale²⁹, R.D. De Souza¹²³, H.F. Degenhardt¹²², A. Deisting^{99,95}, A. Deloff⁷⁹, C. Deplano⁸⁴, P. Dhankher⁴⁷, D. Di Bari³², A. Di Mauro³⁴, P. Di Nezza⁷³, B. Di Ruzza¹⁰⁹, M.A. Diaz Corchero¹⁰, T. Dietel⁹¹, P. Dillenseger⁶⁰, R. Divià³⁴, Ø. Djuvsland²¹, A. Dobrin^{58,34}, D. Domenicis Gimenez¹²², B. Dönigus⁶⁰, O. Dordic²⁰, T. Drozhzhova⁶⁰, A.K. Dubey¹³⁷, A. Dubla⁹⁹, L. Ducroux¹³³, A.K. Duggal⁹⁰, P. Dupieux⁷¹, R.J. Ehlers¹⁴¹, D. Elia¹⁰⁵, E. Endress¹⁰⁴, H. Engel⁵⁹, E. Eppele¹⁴¹, B. Erasmus¹¹⁵, F. Erhardt¹³², B. Espagnon⁵¹, S. Esumi¹³¹, G. Eulisse³⁴, J. Eum⁹⁸, D. Evans¹⁰³, S. Evdokimov¹¹³, L. Fabbietti^{35,96}, D. Fabris¹⁰⁹, J. Faivre⁷², A. Fantoni⁷³, M. Fasel^{87,75}, L. Feldkamp⁶¹, A. Feliciello¹¹², G. Feofilov¹³⁶, J. Ferencei⁸⁶, A. Fernández Téllez², E.G. Ferreira¹⁶, A. Ferretti²⁵, A. Festanti²⁸, V.J.G. Feuillard^{71,65}, J. Figiel¹¹⁹, M.A.S. Figueredo¹²², S. Filchagin¹⁰¹, D. Finogeev⁵², F.M. Fionda²³, E.M. Fiore³², M. Floris³⁴, S. Foertsch⁶⁶, P. Foka⁹⁹, S. Fokin⁸², E. Fragiaco¹¹¹, A. Francescon³⁴, A. Francisco¹¹⁵, U. Frankenfeld⁹⁹, G.G. Fronze²⁵, U. Fuchs³⁴, C. Furget⁷², A. Furs⁵², M. Fusco Girard²⁹, J.J. Gaardhøje⁸³,

M. Gagliardi²⁵, A.M. Gago¹⁰⁴, K. Gajdosova⁸³, M. Gallio²⁵, C.D. Galvan¹²¹, D.R. Gangadharan⁷⁵, P. Ganoti⁷⁸, C. Gao⁷, C. Garabatos⁹⁹, E. Garcia-Solis¹³, K. Garg²⁷, P. Garg⁴⁸, C. Gargiulo³⁴, P. Gasik^{35,96}, E.F. Gauger¹²⁰, M.B. Gay Ducati⁶³, M. Germain¹¹⁵, P. Ghosh¹³⁷, S.K. Ghosh⁴, P. Gianotti⁷³, P. Giubellino^{34,112}, P. Giubilato²⁸, E. Gladysz-Dziadus¹¹⁹, P. Glässel⁹⁵, D.M. Gómez Coral⁶⁴, A. Gomez Ramirez⁵⁹, A.S. Gonzalez³⁴, V. Gonzalez¹⁰, P. González-Zamora¹⁰, S. Gorbunov⁴¹, L. Görlich¹¹⁹, S. Gotovac¹¹⁸, V. Grabski⁶⁴, L.K. Graczykowski¹³⁸, K.L. Graham¹⁰³, L. Greiner⁷⁵, A. Grelli⁵³, C. Grigoras³⁴, V. Grigoriev⁷⁶, A. Grigoryan¹, S. Grigoryan⁶⁷, N. Grion¹¹¹, J.M. Gronefeld⁹⁹, F. Groa³⁰, J.F. Grosse-Oetringhaus³⁴, R. Grosso⁹⁹, L. Gruber¹¹⁴, F.R. Grull⁵⁹, F. Guber⁵², R. Guernane^{34,72}, B. Guerzoni²⁶, K. Gulbrandsen⁸³, T. Gunji¹³⁰, A. Gupta⁹², R. Gupta⁹², I.B. Guzman², R. Haake^{34,61}, C. Hadjidakis⁵¹, H. Hamagaki^{77,130}, G. Hamar¹⁴⁰, J.C. Hamon¹³⁴, J.W. Harris¹⁴¹, A. Harton¹³, D. Hatzifotiadiou¹⁰⁶, S. Hayashi¹³⁰, S.T. Heckel⁶⁰, E. Hellbär⁶⁰, H. Helstrup³⁶, A. Hergelegiu⁸⁰, G. Herrera Corral¹¹, F. Herrmann⁶¹, B.A. Hess⁹⁴, K.F. Hetland³⁶, H. Hillemanns³⁴, B. Hippolyte¹³⁴, J. Hladky⁵⁶, D. Horak³⁸, R. Hosokawa¹³¹, P. Hristov³⁴, C. Hughes¹²⁸, T.J. Humanic¹⁸, N. Hussain⁴³, T. Hussain¹⁷, D. Hutter⁴¹, D.S. Hwang¹⁹, R. Ilkaev¹⁰¹, M. Inaba¹³¹, M. Ippolitov^{82,76}, M. Irfan¹⁷, V. Isakov⁵², M.S. Islam⁴⁸, M. Ivanov^{34,99}, V. Ivanov⁸⁸, V. Izucheev¹¹³, B. Jacak⁷⁵, N. Jacazio²⁶, P.M. Jacobs⁷⁵, M.B. Jadhav⁴⁷, S. Jadlovská¹¹⁷, J. Jadlovsky¹¹⁷, C. Jahnke³⁵, M.J. Jakubowska¹³⁸, M.A. Janik¹³⁸, P.H.S.Y. Jayarathna¹²⁵, C. Jena⁸¹, S. Jena¹²⁵, M. Jercic¹³², R.T. Jimenez Bustamante⁹⁹, P.G. Jones¹⁰³, A. Jusko¹⁰³, P. Kalinak⁵⁵, A. Kalweit³⁴, J.H. Kang¹⁴², V. Kaplin⁷⁶, S. Kar¹³⁷, A. Karasu Uysal⁷⁰, O. Karavichev⁵², T. Karavicheva⁵², L. Karayan^{99,95}, E. Karpechev⁵², U. Kebschull⁵⁹, R. Keidel¹⁴³, D.L.D. Keijdener⁵³, M. Keil³⁴, M. Mohisin Khan^{17,iii}, P. Khan¹⁰², S.A. Khan¹³⁷, A. Khanzadeev⁸⁸, Y. Kharlov¹¹³, A. Khatun¹⁷, A. Khuntia⁴⁸, M.M. Kielbowicz¹¹⁹, B. Kileng³⁶, D.W. Kim⁴², D.J. Kim¹²⁶, D. Kim¹⁴², H. Kim¹⁴², J.S. Kim⁴², J. Kim⁹⁵, M. Kim⁵⁰, M. Kim¹⁴², S. Kim¹⁹, T. Kim¹⁴², S. Kirsch⁴¹, I. Kisel⁴¹, S. Kiselev⁵⁴, A. Kisiel¹³⁸, G. Kiss¹⁴⁰, J.L. Klay⁶, C. Klein⁶⁰, J. Klein³⁴, C. Klein-Bösing⁶¹, S. Klewin⁹⁵, A. Kluge³⁴, M.L. Knichel⁹⁵, A.G. Knospe¹²⁵, C. Kobdaj¹¹⁶, M. Kofarago³⁴, T. Kollegger⁹⁹, A. Kolojvari¹³⁶, V. Kondratiev¹³⁶, N. Kondratyeva⁷⁶, E. Kondratyuk¹¹³, A. Konevskikh⁵², M. Kopcik¹¹⁷, M. Kour⁹², C. Kouzinopoulos³⁴, O. Kovalenko⁷⁹, V. Kovalenko¹³⁶, M. Kowalski¹¹⁹, G. Koyithatta Meethaleveedu⁴⁷, I. Králík⁵⁵, A. Kravčáková³⁹, M. Krivda^{55,103}, F. Krizek⁸⁶, E. Kryshen⁸⁸, M. Krzewicki⁴¹, A.M. Kubera¹⁸, V. Kučera⁸⁶, C. Kuhn¹³⁴, P.G. Kuijer⁸⁴, A. Kumar⁹², J. Kumar⁴⁷, L. Kumar⁹⁰, S. Kumar⁴⁷, S. Kundu⁸¹, P. Kurashvili⁷⁹, A. Kurepin⁵², A.B. Kurepin⁵², A. Kuryakin¹⁰¹, S. Kushpil⁸⁶, M.J. Kweon⁵⁰, Y. Kwon¹⁴², S.L. La Pointe⁴¹, P. La Rocca²⁷, C. Lagana Fernandes¹²², I. Lakomov³⁴, R. Langoy⁴⁰, K. Lapidus¹⁴¹, C. Lara⁵⁹, A. Lardeux^{65,20}, A. Lattuca²⁵, E. Laudi³⁴, R. Lavicka³⁸, L. Lazaridis³⁴, R. Lea²⁴, L. Leardini⁹⁵, S. Lee¹⁴², F. Lehas⁸⁴, S. Lehner¹¹⁴, J. Lehrbach⁴¹, R.C. Lemmon⁸⁵, V. Lenti¹⁰⁵, E. Leogrande⁵³, I. León Monzón¹²¹, P. Lévai¹⁴⁰, S. Li⁷, X. Li¹⁴, J. Lien⁴⁰, R. Lietava¹⁰³, S. Lindal²⁰, V. Lindenstruth⁴¹, C. Lippmann⁹⁹, M.A. Lisa¹⁸, V. Litichevskiy⁴⁵, H.M. Ljunggren³³, W.J. Llope¹³⁹, D.F. Lodato⁵³, P.I. Loenne²¹, V. Loginov⁷⁶, C. Loizides⁷⁵, P. Loncar¹¹⁸, X. Lopez⁷¹, E. López Torres⁹, A. Lowe¹⁴⁰, P. Luettig⁶⁰, M. Lunardon²⁸, G. Luparello²⁴, M. Lupi³⁴, T.H. Lutz¹⁴¹, A. Maevskaya⁵², M. Mager³⁴, S. Mahajan⁹², S.M. Mahmood²⁰, A. Maire¹³⁴, R.D. Majka¹⁴¹, M. Malaev⁸⁸, I. Maldonado Cervantes⁶², L. Malinina^{67,iv}, D. Mal'Kevich⁵⁴, P. Malzacher⁹⁹, A. Mamonov¹⁰¹, V. Manko⁸², F. Manso⁷¹, V. Manzari¹⁰⁵, Y. Mao⁷, M. Marchisone^{66,129}, J. Mareš⁵⁶, G.V. Margagliotti²⁴, A. Margotti¹⁰⁶, J. Margutti⁵³, A. Marín⁹⁹, C. Markert¹²⁰, M. Marquard⁶⁰, N.A. Martin⁹⁹, P. Martinengo³⁴, J.A.L. Martinez⁵⁹, M.I. Martínez², G. Martínez García¹¹⁵, M. Martinez Pedreira³⁴, A. Mas¹²², S. Masciocchi⁹⁹, M. Masera²⁵, A. Masoni¹⁰⁷, A. Mastroserio³², A.M. Mathis^{96,35}, A. Matyja^{128,119}, C. Mayer¹¹⁹, J. Mazer¹²⁸, M. Mazzilli³², M.A. Mazzoni¹¹⁰, F. Meddi²², Y. Melikyan⁷⁶, A. Menchaca-Rocha⁶⁴, E. Meninno²⁹, J. Mercado Pérez⁹⁵, M. Meres³⁷, S. Mhlanga⁹¹, Y. Miake¹³¹, M.M. Mieskolainen⁴⁵, D. Mihaylov⁹⁶, K. Mikhaylov^{54,67}, L. Milano⁷⁵, J. Milosevic²⁰, A. Mischke⁵³, A.N. Mishra⁴⁸, T. Mishra⁵⁷, D. Miśkowiec⁹⁹, J. Mitra¹³⁷, C.M. Mitu⁵⁸, N. Mohammadi⁵³, B. Mohanty⁸¹, E. Montes¹⁰, D.A. Moreira De Godoy⁶¹, L.A.P. Moreno², S. Moretto²⁸, A. Morreale¹¹⁵, A. Morsch³⁴, V. Muccifora⁷³, E. Mudnic¹¹⁸, D. Mühlheim⁶¹, S. Muhuri¹³⁷, M. Mukherjee¹³⁷, J.D. Mulligan¹⁴¹, M.G. Munhoz¹²², K. Munning⁴⁴, R.H. Munzer^{35,60,96}, H. Murakami¹³⁰, S. Murray⁶⁶, L. Musa³⁴, J. Musinsky⁵⁵, C.J. Myers¹²⁵, B. Naik⁴⁷, R. Nair⁷⁹, B.K. Nandi⁴⁷, R. Nania¹⁰⁶, E. Nappi¹⁰⁵, M.U. Naru¹⁵, H. Natal da Luz¹²², C. Nattrass¹²⁸, S.R. Navarro², K. Nayak⁸¹, R. Nayak⁴⁷, T.K. Nayak¹³⁷, S. Nazarenko¹⁰¹, A. Nedosekin⁵⁴, R.A. Negrao De Oliveira³⁴,

L. Nellen⁶², S.V. Nesbo³⁶, F. Ng¹²⁵, M. Nicassio⁹⁹, M. Niculescu⁵⁸, J. Niedziela³⁴, B.S. Nielsen⁸³, S. Nikolaev⁸², S. Nikulin⁸², V. Nikulin⁸⁸, F. Noferini^{106,12}, P. Nomokonov⁶⁷, G. Nooren⁵³, J.C.C. Noris², J. Norman¹²⁷, A. Nyanin⁸², J. Nystrand²¹, H. Oeschler⁹⁵, S. Oh¹⁴¹, A. Ohlson^{95,34}, T. Okubo⁴⁶, L. Olah¹⁴⁰, J. Oleniacz¹³⁸, A.C. Oliveira Da Silva¹²², M.H. Oliver¹⁴¹, J. Onderwaater⁹⁹, C. Oppedisano¹¹², R. Orava⁴⁵, M. Oravec¹¹⁷, A. Ortiz Velasquez⁶², A. Oskarsson³³, J. Otwinowski¹¹⁹, K. Oyama⁷⁷, M. Ozdemir⁶⁰, Y. Pachmayer⁹⁵, V. Pacik⁸³, D. Pagano^{135,25}, P. Pagano²⁹, G. Paic⁶², S.K. Pal¹³⁷, P. Palni⁷, J. Pan¹³⁹, A.K. Pandey⁴⁷, S. Panebianco⁶⁵, V. Papikyan¹, G.S. Pappalardo¹⁰⁸, P. Pareek⁴⁸, J. Park⁵⁰, W.J. Park⁹⁹, S. Parmar⁹⁰, A. Passfeld⁶¹, V. Paticchio¹⁰⁵, R.N. Patra¹³⁷, B. Paul¹¹², H. Pei⁷, T. Peitzmann⁵³, X. Peng⁷, L.G. Pereira⁶³, H. Pereira Da Costa⁶⁵, D. Peresunko^{82,76}, E. Perez Lezama⁶⁰, V. Peskov⁶⁰, Y. Pestov⁵, V. Petráček³⁸, V. Petrov¹¹³, M. Petrovici⁸⁰, C. Petta²⁷, R.P. Pezzi⁶³, S. Piano¹¹¹, M. Pikna³⁷, P. Pillot¹¹⁵, L.O.D.L. Pimentel⁸³, O. Pinazza^{106,34}, L. Pinsky¹²⁵, D.B. Piyarathna¹²⁵, M. Płoskoń⁷⁵, M. Planinic¹³², J. Pluta¹³⁸, S. Pochybova¹⁴⁰, P.L.M. Podesta-Lerma¹²¹, M.G. Poghosyan⁸⁷, B. Polichtchouk¹¹³, N. Poljak¹³², W. Poonsawat¹¹⁶, A. Pop⁸⁰, H. Poppenborg⁶¹, S. Porteboeuf-Houssais⁷¹, J. Porter⁷⁵, J. Pospisil⁸⁶, V. Pozdniakov⁶⁷, S.K. Prasad⁴, R. Preghenella^{34,106}, F. Prino¹¹², C.A. Pruneau¹³⁹, I. Pshenichnov⁵², M. Puccio²⁵, G. Puddu²³, P. Pujahari¹³⁹, V. Punin¹⁰¹, J. Putschke¹³⁹, H. Qvigstad²⁰, A. Rachevski¹¹¹, S. Raha⁴, S. Rajput⁹², J. Rak¹²⁶, A. Rakotozafindrabe⁶⁵, L. Ramello³¹, F. Rami¹³⁴, D.B. Rana¹²⁵, R. Raniwala⁹³, S. Raniwala⁹³, S.S. Räsänen⁴⁵, B.T. Rascanu⁶⁰, D. Rathee⁹⁰, V. Ratza⁴⁴, I. Ravasenga³⁰, K.F. Read^{87,128}, K. Redlich⁷⁹, A. Rehman²¹, P. Reichelt⁶⁰, F. Reidt³⁴, X. Ren⁷, R. Renfordt⁶⁰, A.R. Reolon⁷³, A. Reshetin⁵², K. Reygers⁹⁵, V. Riabov⁸⁸, R.A. Ricci⁷⁴, T. Richert^{53,33}, M. Richter²⁰, P. Riedler³⁴, W. Riegler³⁴, F. Riggi²⁷, C. Ristea⁵⁸, M. Rodríguez Cahuantzi², K. Røed²⁰, E. Rogochaya⁶⁷, D. Rohr⁴¹, D. Röhrich²¹, F. Ronchetti^{73,34}, L. Ronflette¹¹⁵, P. Rosnet⁷¹, A. Rossi²⁸, F. Roukoutakis⁷⁸, A. Roy⁴⁸, C. Roy¹³⁴, P. Roy¹⁰², A.J. Rubio Montero¹⁰, R. Rui²⁴, R. Russo²⁵, E. Ryabinkin⁸², Y. Ryabov⁸⁸, A. Rybicki¹¹⁹, S. Saarinen⁴⁵, S. Sadhu¹³⁷, S. Sadovsky¹¹³, K. Šafařík³⁴, S.K. Saha¹³⁷, B. Sahlmuller⁶⁰, B. Sahoo⁴⁷, P. Sahoo⁴⁸, R. Sahoo⁴⁸, S. Sahoo⁵⁷, P.K. Sahu⁵⁷, J. Saini¹³⁷, S. Sakai^{73,131}, M.A. Saleh¹³⁹, J. Salzwedel¹⁸, S. Sambyal⁹², V. Samsonov^{76,88}, A. Sandoval⁶⁴, D. Sarkar¹³⁷, N. Sarkar¹³⁷, P. Sarma⁴³, M.H.P. Sas⁵³, E. Scapparone¹⁰⁶, F. Scarlassara²⁸, R.P. Scharenberg⁹⁷, C. Schiaua⁸⁰, R. Schicker⁹⁵, C. Schmidt⁹⁹, H.R. Schmidt⁹⁴, M.O. Schmidt⁹⁵, M. Schmidt⁹⁴, J. Schukraft³⁴, Y. Schutz^{115,34,134}, K. Schwarz⁹⁹, K. Schweda⁹⁹, G. Scioli²⁶, E. Scomparin¹¹², R. Scott¹²⁸, M. Šefčík³⁹, J.E. Seger⁸⁹, Y. Sekiguchi¹³⁰, D. Sekihata⁴⁶, I. Selyuzhenkov⁹⁹, K. Senosi⁶⁶, S. Senyukov^{3,134,34}, E. Serradilla^{64,10}, P. Sett⁴⁷, A. Sevcenco⁵⁸, A. Shabanov⁵², A. Shabetai¹¹⁵, O. Shadura³, R. Shahoyan³⁴, A. Shangaraev¹¹³, A. Sharma⁹², A. Sharma⁹⁰, M. Sharma⁹², M. Sharma⁹², N. Sharma^{128,90}, A.I. Sheikh¹³⁷, K. Shigaki⁴⁶, Q. Shou⁷, K. Shtejer^{25,9}, Y. Sibiriak⁸², S. Siddhanta¹⁰⁷, K.M. Sielewicz³⁴, T. Siemiarczuk⁷⁹, D. Silvermyr³³, C. Silvestre⁷², G. Simatovic¹³², G. Simonetti³⁴, R. Singaraju¹³⁷, R. Singh⁸¹, V. Singhal¹³⁷, T. Sinha¹⁰², B. Sitar³⁷, M. Sitta³¹, T.B. Skaali²⁰, M. Slupecki¹²⁶, N. Smirnov¹⁴¹, R.J.M. Snellings⁵³, T.W. Snellman¹²⁶, J. Song⁹⁸, M. Song¹⁴², F. Soramel²⁸, S. Sorensen¹²⁸, F. Sozzi⁹⁹, E. Spiriti⁷³, I. Sputowska¹¹⁹, B.K. Srivastava⁹⁷, J. Stachel⁹⁵, I. Stan⁵⁸, P. Stankus⁸⁷, E. Stenlund³³, J.H. Stiller⁹⁵, D. Stocco¹¹⁵, P. Strmen³⁷, A.A.P. Suaide¹²², T. Sugitate⁴⁶, C. Suire⁵¹, M. Suleymanov¹⁵, M. Suljic²⁴, R. Sultanov⁵⁴, M. Šumbera⁸⁶, S. Sumowidagdo⁴⁹, K. Suzuki¹¹⁴, S. Swain⁵⁷, A. Szabo³⁷, I. Szarka³⁷, A. Szczepankiewicz¹³⁸, M. Szymanski¹³⁸, U. Tabassam¹⁵, J. Takahashi¹²³, G.J. Tambave²¹, N. Tanaka¹³¹, M. Tarhini⁵¹, M. Tariq¹⁷, M.G. Tarzila⁸⁰, A. Tauro³⁴, G. Tejeda Muñoz², A. Telesca³⁴, K. Terasaki¹³⁰, C. Terrevoli²⁸, B. Teyssier¹³³, D. Thakur⁴⁸, S. Thakur¹³⁷, D. Thomas¹²⁰, R. Tieulent¹³³, A. Tikhonov⁵², A.R. Timmins¹²⁵, A. Toia⁶⁰, S. Tripathy⁴⁸, S. Trogolo²⁵, G. Trombetta³², V. Trubnikov³, W.H. Trzaska¹²⁶, B.A. Trzeciak⁵³, T. Tsuji¹³⁰, A. Tumkin¹⁰¹, R. Turrisi¹⁰⁹, T.S. Tveter²⁰, K. Ullaland²¹, E.N. Umaka¹²⁵, A. Uras¹³³, G.L. Usai²³, A. Utrobicic¹³², M. Vala^{117,55}, J. Van Der Maarel⁵³, J.W. Van Hoorne³⁴, M. van Leeuwen⁵³, T. Vanat⁸⁶, P. Vande Vyvre³⁴, D. Varga¹⁴⁰, A. Vargas², M. Vargyas¹²⁶, R. Varma⁴⁷, M. Vasileiou⁷⁸, A. Vasiliev⁸², A. Vauthier⁷², O. Vázquez Doce^{96,35}, V. Vechernin¹³⁶, A.M. Veen⁵³, A. Velure²¹, E. Vercellin²⁵, S. Vergara Limón², R. Vernet⁸, R. Vértesi¹⁴⁰, L. Vickovic¹¹⁸, S. Vigolo⁵³, J. Viinikainen¹²⁶, Z. Vilakazi¹²⁹, O. Villalobos Baillie¹⁰³, A. Villatoro Tello², A. Vinogradov⁸², L. Vinogradov¹³⁶, T. Virgili²⁹, V. Vislavicius³³, A. Vodopyanov⁶⁷, M.A. Völkl⁹⁵, K. Voloshin⁵⁴, S.A. Voloshin¹³⁹, G. Volpe³², B. von Haller³⁴, I. Vorobyev^{96,35}, D. Voscek¹¹⁷, D. Vranic^{34,99}, J. Vrláková³⁹, B. Wagner²¹, J. Wagner⁹⁹, H. Wang⁵³, M. Wang⁷, D. Watanabe¹³¹, Y. Watanabe¹³⁰, M. Weber¹¹⁴, S.G. Weber⁹⁹, D.F. Weiser⁹⁵,

J.P. Wessels⁶¹, U. Westerhoff⁶¹, A.M. Whitehead⁹¹, J. Wiechula⁶⁰, J. Wikne²⁰, G. Wilk⁷⁹, J. Wilkinson⁹⁵, G.A. Willems⁶¹, M.C.S. Williams¹⁰⁶, B. Windelband⁹⁵, W.E. Witt¹²⁸, S. Yalcin⁷⁰, P. Yang⁷, S. Yano⁴⁶, Z. Yin⁷, H. Yokoyama^{131,72}, I-K. Yoo^{34,98}, J.H. Yoon⁵⁰, V. Yurchenko³, V. Zaccolo^{83,112}, A. Zaman¹⁵, C. Zampolli³⁴, H.J.C. Zanolli¹²², S. Zaporozhets⁶⁷, N. Zardoshti¹⁰³, A. Zarochentsev¹³⁶, P. Závada⁵⁶, N. Zaviyalov¹⁰¹, H. Zbroszczyk¹³⁸, M. Zhalov⁸⁸, H. Zhang^{7,21}, X. Zhang^{75,7}, Y. Zhang⁷, C. Zhang⁵³, Z. Zhang⁷, C. Zhao²⁰, N. Zhigareva⁵⁴, D. Zhou⁷, Y. Zhou⁸³, Z. Zhou²¹, H. Zhu^{21,7}, J. Zhu^{7,115}, X. Zhu⁷, A. Zichichi^{12,26}, A. Zimmermann⁹⁵, M.B. Zimmermann^{34,61}, S. Zimmermann¹¹⁴, G. Zinovjev³, J. Zmeskal¹¹⁴

- ¹ A.I. Alikhanyan National Science Laboratory (Yerevan Physics Institute) Foundation, Yerevan, Armenia
- ² Benemérita Universidad Autónoma de Puebla, Puebla, Mexico
- ³ Bogolyubov Institute for Theoretical Physics, Kiev, Ukraine
- ⁴ Bose Institute, Department of Physics and Centre for Astroparticle Physics and Space Science (CAPSS), Kolkata, India
- ⁵ Budker Institute for Nuclear Physics, Novosibirsk, Russia
- ⁶ California Polytechnic State University, San Luis Obispo, CA, United States
- ⁷ Central China Normal University, Wuhan, China
- ⁸ Centre de Calcul de l'IN2P3, Villeurbanne, Lyon, France
- ⁹ Centro de Aplicaciones Tecnológicas y Desarrollo Nuclear (CEADEN), Havana, Cuba
- ¹⁰ Centro de Investigaciones Energéticas Medioambientales y Tecnológicas (CIEMAT), Madrid, Spain
- ¹¹ Centro de Investigación y de Estudios Avanzados (CINVESTAV), Mexico City and Mérida, Mexico
- ¹² Centro Fermi - Museo Storico della Fisica e Centro Studi e Ricerche "Enrico Fermi", Rome, Italy
- ¹³ Chicago State University, Chicago, IL, United States
- ¹⁴ China Institute of Atomic Energy, Beijing, China
- ¹⁵ COMSATS Institute of Information Technology (CIIT), Islamabad, Pakistan
- ¹⁶ Departamento de Física de Partículas and IGFAE, Universidad de Santiago de Compostela, Santiago de Compostela, Spain
- ¹⁷ Department of Physics, Aligarh Muslim University, Aligarh, India
- ¹⁸ Department of Physics, Ohio State University, Columbus, OH, United States
- ¹⁹ Department of Physics, Sejong University, Seoul, South Korea
- ²⁰ Department of Physics, University of Oslo, Oslo, Norway
- ²¹ Department of Physics and Technology, University of Bergen, Bergen, Norway
- ²² Dipartimento di Fisica dell'Università 'La Sapienza' and Sezione INFN, Rome, Italy
- ²³ Dipartimento di Fisica dell'Università and Sezione INFN, Cagliari, Italy
- ²⁴ Dipartimento di Fisica dell'Università and Sezione INFN, Trieste, Italy
- ²⁵ Dipartimento di Fisica dell'Università and Sezione INFN, Turin, Italy
- ²⁶ Dipartimento di Fisica e Astronomia dell'Università and Sezione INFN, Bologna, Italy
- ²⁷ Dipartimento di Fisica e Astronomia dell'Università and Sezione INFN, Catania, Italy
- ²⁸ Dipartimento di Fisica e Astronomia dell'Università and Sezione INFN, Padova, Italy
- ²⁹ Dipartimento di Fisica 'E.R. Caianiello' dell'Università and Gruppo Collegato INFN, Salerno, Italy
- ³⁰ Dipartimento DISAT del Politecnico and Sezione INFN, Turin, Italy
- ³¹ Dipartimento di Scienze e Innovazione Tecnologica dell'Università del Piemonte Orientale and INFN Sezione di Torino, Alessandria, Italy
- ³² Dipartimento Interateneo di Fisica 'M. Merlin' and Sezione INFN, Bari, Italy
- ³³ Division of Experimental High Energy Physics, University of Lund, Lund, Sweden
- ³⁴ European Organization for Nuclear Research (CERN), Geneva, Switzerland
- ³⁵ Excellence Cluster Universe, Technische Universität München, Munich, Germany
- ³⁶ Faculty of Engineering, Bergen University College, Bergen, Norway
- ³⁷ Faculty of Mathematics, Physics and Informatics, Comenius University, Bratislava, Slovakia
- ³⁸ Faculty of Nuclear Sciences and Physical Engineering, Czech Technical University in Prague, Prague, Czech Republic
- ³⁹ Faculty of Science, P.J. Šafárik University, Košice, Slovakia
- ⁴⁰ Faculty of Technology, Buskerud and Vestfold University College, Tonsberg, Norway
- ⁴¹ Frankfurt Institute for Advanced Studies, Johann Wolfgang Goethe-Universität Frankfurt, Frankfurt, Germany
- ⁴² Gangneung-Wonju National University, Gangneung, South Korea
- ⁴³ Gauhati University, Department of Physics, Guwahati, India
- ⁴⁴ Helmholtz-Institut für Strahlen- und Kernphysik, Rheinische Friedrich-Wilhelms-Universität Bonn, Bonn, Germany
- ⁴⁵ Helsinki Institute of Physics (HIP), Helsinki, Finland
- ⁴⁶ Hiroshima University, Hiroshima, Japan
- ⁴⁷ Indian Institute of Technology Bombay (IIT), Mumbai, India
- ⁴⁸ Indian Institute of Technology Indore, Indore, India
- ⁴⁹ Indonesian Institute of Sciences, Jakarta, Indonesia
- ⁵⁰ Inha University, Incheon, South Korea
- ⁵¹ Institut de Physique Nucléaire d'Orsay (IPNO), Université Paris-Sud, CNRS-IN2P3, Orsay, France
- ⁵² Institute for Nuclear Research, Academy of Sciences, Moscow, Russia
- ⁵³ Institute for Subatomic Physics of Utrecht University, Utrecht, Netherlands
- ⁵⁴ Institute for Theoretical and Experimental Physics, Moscow, Russia
- ⁵⁵ Institute of Experimental Physics, Slovak Academy of Sciences, Košice, Slovakia
- ⁵⁶ Institute of Physics, Academy of Sciences of the Czech Republic, Prague, Czech Republic
- ⁵⁷ Institute of Physics, Bhubaneswar, India
- ⁵⁸ Institute of Space Science (ISS), Bucharest, Romania
- ⁵⁹ Institut für Informatik, Johann Wolfgang Goethe-Universität Frankfurt, Frankfurt, Germany
- ⁶⁰ Institut für Kernphysik, Johann Wolfgang Goethe-Universität Frankfurt, Frankfurt, Germany
- ⁶¹ Institut für Kernphysik, Westfälische Wilhelms-Universität Münster, Münster, Germany
- ⁶² Instituto de Ciencias Nucleares, Universidad Nacional Autónoma de México, Mexico City, Mexico
- ⁶³ Instituto de Física, Universidade Federal do Rio Grande do Sul (UFRGS), Porto Alegre, Brazil
- ⁶⁴ Instituto de Física, Universidad Nacional Autónoma de México, Mexico City, Mexico
- ⁶⁵ IRFU, CEA, Université Paris-Saclay, F-91191 Gif-sur-Yvette, France, Saclay, France
- ⁶⁶ iThemba LABS, National Research Foundation, Somerset West, South Africa

- ⁶⁷ Joint Institute for Nuclear Research (JINR), Dubna, Russia
- ⁶⁸ Konkuk University, Seoul, South Korea
- ⁶⁹ Korea Institute of Science and Technology Information, Daejeon, South Korea
- ⁷⁰ KTO Karatay University, Konya, Turkey
- ⁷¹ Laboratoire de Physique Corpusculaire (LPC), Clermont Université, Université Blaise Pascal, CNRS-IN2P3, Clermont-Ferrand, France
- ⁷² Laboratoire de Physique Subatomique et de Cosmologie, Université Grenoble-Alpes, CNRS-IN2P3, Grenoble, France
- ⁷³ Laboratori Nazionali di Frascati, INFN, Frascati, Italy
- ⁷⁴ Laboratori Nazionali di Legnaro, INFN, Legnaro, Italy
- ⁷⁵ Lawrence Berkeley National Laboratory, Berkeley, CA, United States
- ⁷⁶ Moscow Engineering Physics Institute, Moscow, Russia
- ⁷⁷ Nagasaki Institute of Applied Science, Nagasaki, Japan
- ⁷⁸ National and Kapodistrian University of Athens, Physics Department, Athens, Greece
- ⁷⁹ National Centre for Nuclear Studies, Warsaw, Poland
- ⁸⁰ National Institute for Physics and Nuclear Engineering, Bucharest, Romania
- ⁸¹ National Institute of Science Education and Research, Bhubaneswar, India
- ⁸² National Research Centre Kurchatov Institute, Moscow, Russia
- ⁸³ Niels Bohr Institute, University of Copenhagen, Copenhagen, Denmark
- ⁸⁴ Nikhef, Nationaal instituut voor subatomaire fysica, Amsterdam, Netherlands
- ⁸⁵ Nuclear Physics Group, STFC Daresbury Laboratory, Daresbury, United Kingdom
- ⁸⁶ Nuclear Physics Institute, Academy of Sciences of the Czech Republic, Řež u Prahy, Czech Republic
- ⁸⁷ Oak Ridge National Laboratory, Oak Ridge, TN, United States
- ⁸⁸ Petersburg Nuclear Physics Institute, Gatchina, Russia
- ⁸⁹ Physics Department, Creighton University, Omaha, NE, United States
- ⁹⁰ Physics Department, Panjab University, Chandigarh, India
- ⁹¹ Physics Department, University of Cape Town, Cape Town, South Africa
- ⁹² Physics Department, University of Jammu, Jammu, India
- ⁹³ Physics Department, University of Rajasthan, Jaipur, India
- ⁹⁴ Physikalisches Institut, Eberhard Karls Universität Tübingen, Tübingen, Germany
- ⁹⁵ Physikalisches Institut, Ruprecht-Karls-Universität Heidelberg, Heidelberg, Germany
- ⁹⁶ Physik Department, Technische Universität München, Munich, Germany
- ⁹⁷ Purdue University, West Lafayette, IN, United States
- ⁹⁸ Pusan National University, Pusan, South Korea
- ⁹⁹ Research Division and ExtreMe Matter Institute EMMI, GSI Helmholtzzentrum für Schwerionenforschung GmbH, Darmstadt, Germany
- ¹⁰⁰ Rudjer Bošković Institute, Zagreb, Croatia
- ¹⁰¹ Russian Federal Nuclear Center (VNIIEF), Sarov, Russia
- ¹⁰² Saha Institute of Nuclear Physics, Kolkata, India
- ¹⁰³ School of Physics and Astronomy, University of Birmingham, Birmingham, United Kingdom
- ¹⁰⁴ Sección Física, Departamento de Ciencias, Pontificia Universidad Católica del Perú, Lima, Peru
- ¹⁰⁵ Sezione INFN, Bari, Italy
- ¹⁰⁶ Sezione INFN, Bologna, Italy
- ¹⁰⁷ Sezione INFN, Cagliari, Italy
- ¹⁰⁸ Sezione INFN, Catania, Italy
- ¹⁰⁹ Sezione INFN, Padova, Italy
- ¹¹⁰ Sezione INFN, Rome, Italy
- ¹¹¹ Sezione INFN, Trieste, Italy
- ¹¹² Sezione INFN, Turin, Italy
- ¹¹³ SSC IHEP of NRC Kurchatov institute, Protvino, Russia
- ¹¹⁴ Stefan Meyer Institut für Subatomare Physik (SMI), Vienna, Austria
- ¹¹⁵ SUBATECH, Ecole des Mines de Nantes, Université de Nantes, CNRS-IN2P3, Nantes, France
- ¹¹⁶ Suranaree University of Technology, Nakhon Ratchasima, Thailand
- ¹¹⁷ Technical University of Košice, Košice, Slovakia
- ¹¹⁸ Technical University of Split FESB, Split, Croatia
- ¹¹⁹ The Henryk Niewodniczanski Institute of Nuclear Physics, Polish Academy of Sciences, Cracow, Poland
- ¹²⁰ The University of Texas at Austin, Physics Department, Austin, TX, United States
- ¹²¹ Universidad Autónoma de Sinaloa, Culiacán, Mexico
- ¹²² Universidade de São Paulo (USP), São Paulo, Brazil
- ¹²³ Universidade Estadual de Campinas (UNICAMP), Campinas, Brazil
- ¹²⁴ Universidade Federal do ABC, Santo Andre, Brazil
- ¹²⁵ University of Houston, Houston, TX, United States
- ¹²⁶ University of Jyväskylä, Jyväskylä, Finland
- ¹²⁷ University of Liverpool, Liverpool, United Kingdom
- ¹²⁸ University of Tennessee, Knoxville, TN, United States
- ¹²⁹ University of the Witwatersrand, Johannesburg, South Africa
- ¹³⁰ University of Tokyo, Tokyo, Japan
- ¹³¹ University of Tsukuba, Tsukuba, Japan
- ¹³² University of Zagreb, Zagreb, Croatia
- ¹³³ Université de Lyon, Université Lyon 1, CNRS-IN2P3, IPN-Lyon, Villeurbanne, Lyon, France
- ¹³⁴ Université de Strasbourg, CNRS, IPHC UMR 7178, F-67000 Strasbourg, France
- ¹³⁵ Università di Brescia, Brescia, Italy
- ¹³⁶ V. Fock Institute for Physics, St. Petersburg State University, St. Petersburg, Russia
- ¹³⁷ Variable Energy Cyclotron Centre, Kolkata, India
- ¹³⁸ Warsaw University of Technology, Warsaw, Poland
- ¹³⁹ Wayne State University, Detroit, MI, United States
- ¹⁴⁰ Wigner Research Centre for Physics, Hungarian Academy of Sciences, Budapest, Hungary
- ¹⁴¹ Yale University, New Haven, CT, United States
- ¹⁴² Yonsei University, Seoul, South Korea
- ¹⁴³ Zentrum für Technologietransfer und Telekommunikation (ZTT), Fachhochschule Worms, Worms, Germany

- ⁱ Deceased.
- ⁱⁱ Also at: Georgia State University, Atlanta, Georgia, United States.
- ⁱⁱⁱ Also at: Department of Applied Physics, Aligarh Muslim University, Aligarh, India.
- ^{iv} Also at: M.V. Lomonosov Moscow State University, D.V. Skobeltsyn Institute of Nuclear Physics, Moscow, Russia.